Frustration-induced highly anisotropic magnetic patterns in the classical XY model on the kagome lattice

Alexei Andreanov[1,2] and M. V. Fistul[1,2,3,4]

[1]*Center for Theoretical Physics of Complex Systems, Institute for Basic Science (IBS), Daejeon 34126, Korea*
[2]*Basic Science Program, Korea University of Science and Technology (UST), Daejeon 34113, Korea*
[3]*Theoretische Physik III, Ruhr-University Bochum, Bochum 44801, Germany*
[4]*Russian Quantum Center, National University of Science and Technology "MISIS," 119049 Moscow, Russia*

We predict and observe numerically highly anisotropic magnetic patterns in the classical frustrated model of planar XY spins on the regular kagome lattice. Frustration is introduced by a specific spatial arrangement of both ferromagnetic and antiferromagnetic bonds between adjacent magnetic moments on the lattice vertices. Defining a quantitative measure of frustration, we find that at a critical value of frustration, $f = f_c = 3/4$, the system displays a phase transition from an ordered ferromagnetic state to a frustrated regime featuring a highly degenerate ground state. In this frustrated regime, which extends for a finite range of frustrations $f_c < f \leqslant 1$, we obtain an unexpected scaling of a spatially averaged magnetization $\langle \vec{M} \rangle$ with the total number of nodes N: $\langle \vec{M} \rangle \simeq N^{-1/4}$. This scaling results from highly anisotropic magnetic patterns displaying perfect ferromagnetic ordering along the y-direction, and short-range correlations of magnetic moments along the x-direction. We show that all these features are explained by the presence of the doubly degenerate ground state in the basic cell, i.e., a single triangle, of the kagome lattice combined with an extensive number of intrinsic constraints on the spins. This model represents an interesting class of frustrated magnetic systems, which might be present in other lattice geometries.

Introduction. Low-dimensional frustrated magnetic systems composed of strongly interacting microscopic magnetic moments located on vertices of regular lattices have fascinated scientists for many years. Multiple magnetic phases, e.g., simple ferromagnetic or antiferromagnetic states, as well as highly degenerate ground states with exotic properties [1–3], topological magnetic vortices and magnetic vortex-(anti)vortex pairs [4,5], and magnetic skyrmions [6], to name a few, as well as the corresponding phase transitions have been predicted theoretically and observed experimentally [7–9]. Similar inhomogeneous states have been predicted and observed in other settings, such as various artificially prepared solid states and optical systems, e.g., Josephson junction networks [10–13], trapped-ion simulators [14], and/or photonic crystals [15,16] thanks to the universality of the underlying mathematical models describing these magnetic phases.

Systems of strongly interacting planar magnetic moments defined on various quasi-one-dimensional (quasi-1D) or 2D lattices, the so-called *classical XY model*, are a case of special interest, hosting both spin-waves and topological excitations, and the famous Berezinskii-Kosterlitz-Thouless (BKT) transition [4,5]. Even more peculiar inhomogeneous magnetic patterns have been obtained in the ground state of *frustrated* magnetic lattices [17–20], e.g., the vortex states, the checkerboard distribution of vortices [10,21], strip phases [22], etc., and sharp transitions were observed between these magnetic patterns as the external parameter varies. This abundance of different ground states is a

consequence of frustrations that in these systems can be introduced by various means: application of an external magnetic field [23–25]; fabrication of specific geometry such as honeycomb, Lieb, or kagome lattices [10,17]; and periodic patterns of magnetic couplings with alternating signs (ferromagnetic/antiferromagnetic interactions) [19,26]. Identifying the ground states in such settings is an intriguing problem requiring a combination of analytical and numerical tools.

In this paper, we consider a classical frustrated XY model on the kagome lattice. Our analysis relies on a corner-sharing property of the kagome lattice: every site is shared in between two triangles of the lattice (see Fig. 1). Frustration in this model arises due to periodically distributed magnetic couplings with alternating signs. We find and classify highly degenerate ground states occurring for large enough frustration. These ground states exhibit extremely anisotropic magnetic patterns that are characterized by spatial correlation functions. The fingerprint of the patterns is the unusual scaling of the spatially averaged magnetization with the system size.

A great advantage of this method of introducing the frustration is the persistence of the frustrated regime and the corresponding complex ground state for a finite range of couplings rather than for a specific fine-tuned value of couplings, as was discussed in many previous works [2,10,24,25]. A related frustration regime was explored in detail in Ref. [27] for the case of Josephson junction networks forming 1D diamond and sawtooth chains. Two phases—ferromagnetic ordering
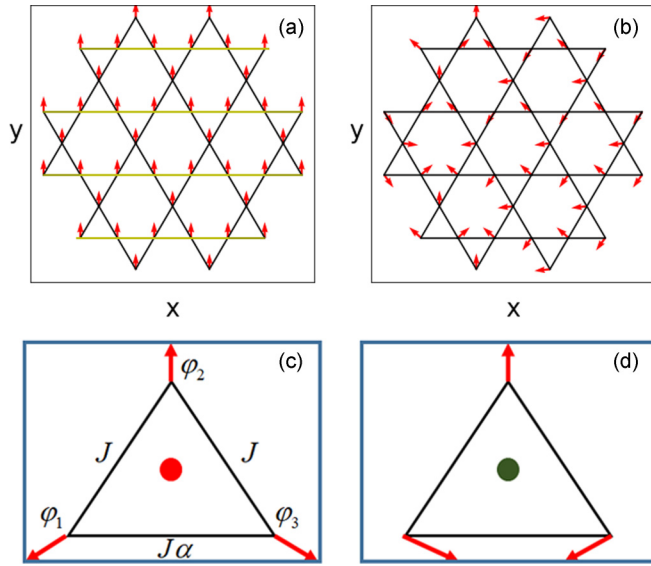
FIG. 1. (a), (b) The classical anisotropic XY model on the kagome lattice. The color code of the links—black for FM and dark yellow for α-links—in (a) shows the anisotropic distribution of the couplings. Parts (a) and (b) show nonfrustrated/ferromagnetic/$f = 0$ and frustrated/$f = 1$ ground states. (c), (d) Magnetic moments of a single triangle in the frustrated ($f > 0.75$) phase. The two possible configurations of the phases $\phi_{i=1,2,3}$—clockwise (counterclockwise)—are marked by red (green) circles. The couplings J and $J\alpha$ are indicated for the single triangle.

and a disordered pattern of penetrating vortices (antivortices) separated by a $T = 0$ phase transition—have been found.

Such a classical frustrated XY model can be naturally implemented in artificially prepared Josephson junctions networks [11–13] and would require Josephson couplings of different signs. Such Josephson couplings are provided by the so-called π-Josephson junctions that can be fabricated on the basis of multijunction superconducting quantum interference devices (SQUIDs) in an externally applied magnetic field [10–13,28,29], superconductor-ferromagnet-superconductor junctions [30], different facets of grain boundaries of high-temperature superconductors [31], or Josephson junctions between two-band superconductors [32].

The model. We consider N planar spins $\vec{s}_i = (\cos \varphi_i, \sin \varphi_i)$ sitting at the vertices of a finite patch of the kagome lattice with lattice spacing $a = 1$. The Hamiltonian is

$$\mathcal{H} = -J \sum_{\langle ij \rangle} \alpha_{ij} \vec{s}_i \cdot \vec{s}_j = -J \sum_{\langle ij \rangle} \alpha_{ij} \cos(\varphi_i - \varphi_j), \quad (1)$$

where J is the strength of the interaction, which we set to 1, and α_{ij} is the coupling, which we take to be nearest-neighbor. The frustration is introduced as follows: $\alpha_{ij} = \alpha$ for all the *horizontal* links (e.g., pointing along the x-direction) and $\alpha_{ij} = 1$ for all the other links. The coupling strength α varies from 1 to -1. In our conventions, the positive (negative) coupling corresponds to ferromagnetic (antiferromagnetic) interaction. To quantify frustration, we define the frustration parameter $f = (1 - \alpha)/2$, so that for frustrations $0 \leqslant f \leqslant 0.5$ all the links are ferromagnetic ones, while for frustrations $0.5 < f \leqslant 1$ there are both ferromagnetic (FM) and antifer-

romagnetic (AFM) couplings with a periodic pattern in space. Before discussing the case of generic frustration f, we remark that exactly for frustration $f = 1$ ($\alpha = -1$) our model can be mapped onto the well-known kagome XY antiferromagnet [33]. This is a consequence of a special symmetry of our Hamiltonian (1): flipping all the spins $\vec{s} \to -\vec{s}$ that only have ferromagnetic adjacent links and then changing the sign of all the FM links does not change the energy of the state, while the Hamiltonian becomes that of the antiferromagnetic kagome Ising model. The pattern of the FM and AFM couplings and the two representative ground states for low and high frustrations are shown in Figs. 1(a) and 1(b), respectively.

The Hamiltonian (1) expressed in the angles φ_i representation [5,10,34,35] also describes the dynamics of complex Josephson junction networks composed of both 0- and π-junctions [30–32]. For these networks, the parameter $J\alpha_{ij}$ represents the critical current of a single Josephson junction between the superconducting islands occupying the lattice nodes i and j.

Ground state. Next we discuss the zero-temperature ($T = 0$) phase diagram, i.e., the ground state of a system, as a function of frustration f: for low values of frustration, $f < f_c = 3/4$, there is a unique FM ground state. However, it becomes unstable for high values of frustrations, $f > f_c$, as first indicated by the appearance of an unstable flatband mode in the spin-wave spectrum, similarly to quasi-one-dimensional cases, e.g., the frustrated sawtooth and diamond chains, studied in Ref. [27]. Such a flatband mode indicates instability of the FM ground state toward a new highly degenerated set of ground states. One such ground state is shown in Fig. 1(b). Just like in sawtooth and diamond chains [27], we observe that the ground states (GSs) of the Hamiltonian (1) minimize the energy of individual triangles of the kagome lattice due to the corner-sharing character of the lattice. A single triangle has two FM links and one AFM link for high frustrations, and it has *two degenerate GSs* for large frustration, $f_c < f < 1$. The corresponding two sets of phases $\varphi_{1,2,3}$ are [27] [as shown in Figs. 1(c) and 1(d)]

$$\varphi_2 - \varphi_1 = \varphi_3 - \varphi_2 = u_{\pm}, \quad \varphi_3 - \varphi_1 = 2u_{\pm},$$

$$u_{\pm} = \pm 2 \arccos \left[\frac{1}{4f - 2} \right]. \quad (2)$$

The two solutions correspond to the penetration of a vortex (antivortex) that differs by clockwise (counterclockwise) rotation of the magnetic moments $\vec{s}_{1-3}$ on the triangle in the Josephson junction terminology. The vortices (antivortices) are marked by red (green) circles in Figs. 1(c) and 1(d).

In the frustrated regime, $f_c < f \leqslant 1$, the full set of ground states is given by the set of all the possible tilings of the triangles of the kagome lattice with these two states of a single triangle. These tilings have to satisfy a macroscopic number of intrinsic constraints: the sums of phases φ_i around any closed loop made of the hexagons of the kagome lattice have to be $2\pi n$, where $n = 0, \pm 1, \dots$. This can be simplified by imposing this constraint for individual hexagons only. In the spin language, the ground states have total spin of every triangle fixed to have the same length, as implied by the configurations (2) but different directions. This is different from many frustrated magnetic models, where the typical constraint

requires a zero total spin of every triangle or other frustrated unit [2,36].

To study GS phase configurations for finite kagome lattices, we implemented a transfer-matrix-like algorithm that generates ground states satisfying these constraints. It proceeds by scanning through the kagome lattice from bottom to top, and assigning the phases to the sites of the hexagons based on the constraints. We have implemented a stochastic version of this algorithm, which produces random samples of the ground-state manifold, and we used it to generate representative samples of the ground-state manifold for a wide range of lattice sizes. We also used this stochastic sampling for small lattice sizes to count the number of ground states by running the sampling until no new ground states were discovered. These enumeration results suggest the scaling of the total number of eigenstates $\mathcal{N}_{\mathrm{GS}}$ as $\ln \mathcal{N}_{\mathrm{GS}} \propto \sqrt{N}$. This highlights an important role played by the local constraints discussed above since in their absence where the triangles can be tiled freely with any of the configurations (2), we would have $\ln \mathcal{N}_{\mathrm{GS}} \propto N$. This is exactly the situation in the 1D case of the sawtooth or diamond chains [27].

Magnetization and spatial correlation functions. Next we discuss the properties of the ground states of the model at temperature $T = 0$: the average magnetization $\langle M \rangle = \frac{1}{N} |\sum_i \vec{s}_i|$ and the correlation function $C(i - j) = \langle \vec{s}_i \vec{s}_j \rangle$. The dependence of the magnetization $\langle M \rangle$ on frustration f is shown in Fig. 2(a): Magnetization is completely saturated taking the largest possible value $M = 1$ for small frustrations $0 < f < f_c$, where the ground state is ferromagnetic, and it does not depend on either N or f. For large frustrations $f > f_c$ the average magnetization $\langle M \rangle$ shows a strong dependence on frustration f and the number of sites N. In the limit of $N \to \infty$, the magnetization flows to zero for all $f > f_c$, indicating the presence of disordered magnetic patterns. The dependence of the magnetization on the number of sites N is presented in Fig. 2(b): for small values of N there is a noticeable magnetization that flows to zero as N increases for all values of frustration $f > f_c$. However, in order to see that, one has to go to larger and larger system sizes as one approaches the critical frustration f_c.

We quantitatively relate the size dependence of the magnetization $\langle M \rangle$ to the spatial correlation functions. For a large number of sites $N \gg 1$ we can use the continuous limit, and introducing the spatial correlation function $C(\vec{\rho}) = \langle \vec{s}(\vec{\rho}) \cdot \vec{s}(0) \rangle$, the magnetization is expressed as

$$\langle M^2 \rangle = \frac{1}{L^2} \int d^2 \vec{\rho} \, C(\vec{\rho}), \qquad (3)$$

where $L \simeq \sqrt{N}$ is the linear size of a system. Thus, the dependence of $\langle M \rangle = \sqrt{\langle M^2 \rangle}$ on the size L (or the number of sites N) is completely determined by the correlation function $C(\vec{\rho})$. Assuming an isotropic correlation function with a finite frustration-dependent correlation length $\xi(f)$, we obtain $\langle M \rangle \propto 1/\sqrt{N}$ as $L \gg \xi$. This scaling is confirmed for the same model on the sawtooth chain [27] [dashed line in Fig. 2(b)]. However, the scaling of the magnetization $\langle M \rangle \propto N^{-1/4}$ observed on the kagome lattice for various large values of frustrations is clearly different [solid lines in Fig. 2(b)]. Such scaling suggests a *strong anisotropy* of the correlation
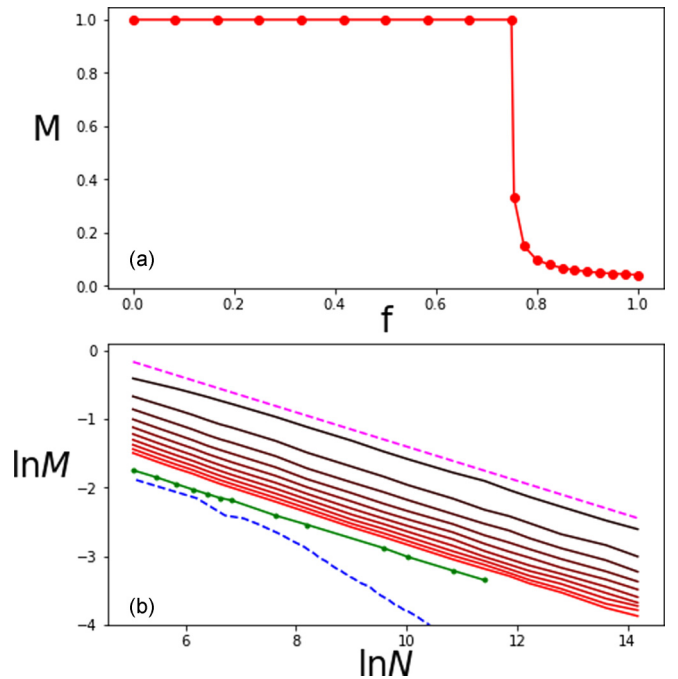

FIG. 2. Average magnetization $\langle M \rangle$ of the XY model. (a) The dependence of the magnetization on frustration f for $N = 90\,300$ spins: in the frustrated phase the magnetization drops to zero. The nonzero values of the magnetization, especially for $f \gtrsim f_c$, are a finite-size effect. (b) Average magnetization as a function of the system size L for several frustrations—0.755 to 1.0 (solid lines: the brighter the color, the larger the frustration; frustration increases as the color goes from black to red/from the top to the bottom curve). Several other curves are shown for comparison: the dashed magenta line is the $M \propto N^{-1/4}$ dependence. The dashed blue curve shows the average magnetization $\langle M \rangle$ of the frustrated sawtooth chain [27] vs the system size L, while the solid green line corresponds to the kagome AF case of $f = 1$.

function $C(\vec{\rho})$ in the frustrated regime. Namely, such scaling $\langle M \rangle \propto N^{-1/4}$ for high frustrations can be explained assuming long-range correlations in one direction, and short-range correlations in the perpendicular direction.

To check this hypothesis, we calculated the spatial correlation function $C_{x,y}(\vec{\rho})$ numerically for several values of frustration and for two different directions, x (horizontal) and y (vertical). The typical behavior of the correlation functions is presented in Fig. 3 for $f = 4/5$ and two different system sizes (the other values of $f > f_c$ show similar behavior). We see indeed a strong anisotropy in the spatial correlation functions: short-range exponential correlations along the horizontal direction [see the $C_x(\vec{\rho})$ in Fig. 3(a)], and long-range ferromagnetic correlations along the vertical direction [see the $C_y(\vec{\rho})$ in Fig. 3(b)]. The exponential decay of the correlation function along the horizontal direction is confirmed in the inset of Fig. 3(a), which shows the log-normal plot. Two comments are in order. First, the long-range ferromagnetic correlations in the y direction were observed for systems of large size; for systems of moderate size, i.e., $N \simeq 2000$ [red (gray) dots in Fig. 3(b)], the long-range correlations are absent. Secondly, the correlation length of $C_x(\vec{\rho})$ increases as the frustration f approaches the critical value of f_c, and this
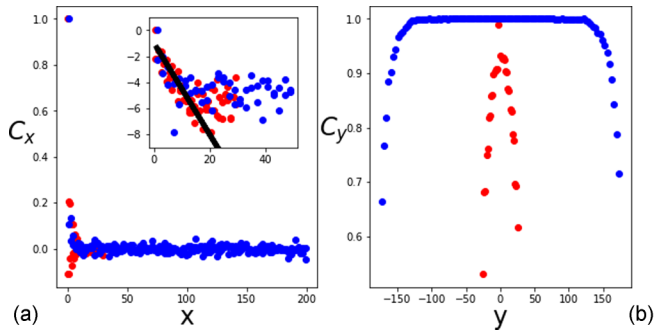
FIG. 3. The anisotropic spin-spin correlators $C_{x,y}(i-j)$ in the frustrated phase for frustration $f = 4/5$ and two system sizes $N = 2070$ [red (gray)] and $N = 90\,300$ [blue (light gray)]. (a) Short-range correlations along the x-direction. The inset shows the same plot in the log scale: the thick black line is the exponential decay provided for reference. (b) Emerging long-range ferromagnetic correlations along the y-direction: as the system size increases, the ferromagnetic plateau is emerging.

enhancement of the correlation length explains the saturation effect in the dependence of $\ln\langle M \rangle$ on N observed in the region of small N [see Fig. 2(b)].

Discussion. Here, we present a qualitative explanation of this highly anisotropic behavior of the correlation functions based on the analysis of the degenerate ground states. We start with a single hexagon of the kagome lattice composed of six triangles and having one closed loop. The ground states of this hexagon are all the possible configurations (2) of individual triangles subject to the constraint of zero-phase accumulation over the hexagon loop. This gives the 14-times degenerate ground state. The seven GSs are shown in Figs. 1(a)–1(g), and the remaining seven GSs are obtained by swapping red and green marks, corresponding to the two possible ground states of individual triangles. It is worth pointing out that the total number of tilings is $2^6 = 64$, and therefore even a single constraint drastically reduces the number of available states. Out of these 14 configurations, 8 show perfect anisotropy in the vertical direction, while the remaining 6 are more isotropic. For larger system sizes, the fraction of ground states that show no anisotropy drops down, and the overwhelming number of ground states has the almost perfect ferromagnetic ordering in the vertical direction. This results in the anisotropic behavior of the correlation function $C_{x,y}(i-j)$ that we discussed above (see Fig. 3). The perfect correlations in the vertical direction drop down in a layer at the boundary. The thickness of this layer does not scale with the total number of sites N.

This argument also provides a simple intuitive explanation of the $\sqrt{N}$ scaling of the logarithm of the number of ground states $\ln \mathcal{N}_{\mathrm{GS}}$: in the presence of the perfect correlations in the vertical direction, the degeneracy is only coming from the horizontal direction, and it scales with the horizontal extent of the system, which is exactly $\sqrt{N}$ for a system of N spins.

As we have stated above, the ground state of the model has the total phase accumulation of phase over any hexagon proportional to $2\pi n$ with integer n. Our analysis shows that for most values of frustration f only the constraints with the value $n = 0$ are realized in the ground states. The ground-state realizations corresponding to the sums of phases φ_i

on closed loops around the hexagons $\pm 2\pi$ were obtained for special values of frustration $f = (\sqrt{3} + 3)/6$ and $f = 1$. These additional realizations can lead to the recovering of the isotropic spatial correlation function $C_{x,y}(\vec{\rho})$. However, e.g., for $f = 1$ the spatial isotropic correlation function shows long-range correlations as $C(\rho) \simeq 1/\rho$, and the spatially averaged magnetization still displays the scaling $\langle \vec{M} \rangle \simeq N^{-1/4}$ [see Fig. 2(b)].

So far we have concentrated on the $T = 0$ ground states, which exhibit a degeneracy. In general, such degeneracies are susceptible to various perturbations that might lift the degeneracy. In the case of the thermal (or quantum) fluctuations, such degeneracy lifting is known as *order-by-disorder* [37]. To explore this possibility, we have used the standard approach [36] and analyzed the Gaussian fluctuations around the ground states corresponding to the limit of low temperatures: Expanding the free energy $F(T \to 0)$ to quadratic order in the fluctuations $\varphi_{i,\mathrm{GS}} + \delta\varphi_i$, one computes the temperature-dependent correction to the ground-state energy. Order-by-disorder is indicated by the dependence of the correction on the ground-state realization. We have found no sign of any thermal order-by-disorder selection to the harmonic order for all values of $f > f_c$. We have also found zero modes, their number being proportional to the system size N. However, a more careful analysis indicates that this is a finite-size effect caused by the open boundary used in the simulations. The location of the weight of the eigenmodes associated with the zero modes scales with the system size, indicating that the modes are located close to the boundary.

Conclusions. We have studied various magnetic patterns in the model of frustrated planar interacting magnetic moments (the classical XY model) on the kagome lattice. The frustration is provided by the presence of both ferromagnetic and antiferromagnetic interactions between adjacent magnetic moments. At the critical value of the frustration,
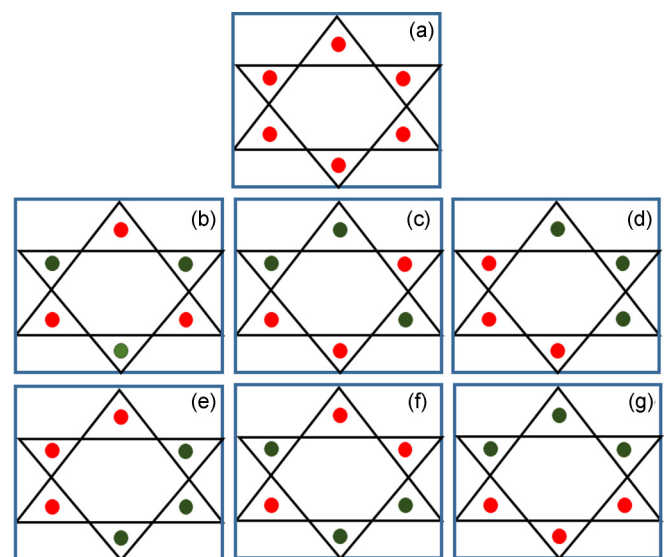

FIG. 4. (a)–(g) Distributions of magnetic moments in a single plaquette of the kagome lattice. The (counterclockwise) clockwise distributions of a single triangle magnetic moment $\vec{M}_{1-3}$ are marked by (green) red circles.

$f = f_c = 3/4$, such a system shows the phase transition from the ordered ferromagnetic state to the disordered frustration regime characterized by a highly degenerate ground state [see Fig. 2(a)]. In this frustrated regime, $f_c < f \leqslant 1$, unexpected scaling of spatially averaged magnetization $\langle M \rangle$ on the number of sites, N, i.e., $\langle M \rangle \simeq N^{-1/4}$, has been obtained [see Fig. 2(b)]. Such scaling is determined by the anisotropic magnetic patterns displaying the ferromagnetic ordering along the y-direction, and short-range correlations of magnetic moments along the x-direction (see Fig. 3). All of these intriguing features were explained by the presence of a doubly degenerate ground state of a basic cell, i.e., single triangles, of the kagome lattice [see Figs. 1(c) and 1(d)] accompanying a large amount of intrinsic constraints [see Figs. 4(a)–4(g)].

The classical frustrated XY model on the kagome lattice can be implemented in natural magnetic molecular clusters, artificially prepared Josephson junctions networks, and photonic crystals, and we anticipate the observation of the frustration-induced phase transition and various anisotropic magnetic patterns in such systems. An interesting open problem is to understand how this frustrated degenerate phase reacts to various perturbations, like dilution, which is known to produce interesting effects in other strongly frustrated systems [38–41].

[1] R. Moessner and J. T. Chalker, Low-temperature properties of classical geometrically frustrated antiferromagnets, Phys. Rev. B **58**, 12049 (1998).

[2] C. L. Henley, The "coulomb phase" in frustrated systems, Annu. Rev. Condens. Matter Phys. **1**, 179 (2010).

[3] C. Castelnovo, R. Moessner, and S. L. Sondhi, Magnetic monopoles in spin ice, Nature (London) **451**, 42 (2008).

[4] J. V. José, *40 Years of Berezinskii-Kosterlitz-Thouless Theory* (World Scientific, Singapore, 2013).

[5] J. V. José, L. P. Kadanoff, S. Kirkpatrick, and D. R. Nelson, Renormalization, vortices, and symmetry-breaking perturbations in the two-dimensional planar model, Phys. Rev. B **16**, 1217 (1977).

[6] N. Nagaosa and Y. Tokura, Topological properties and dynamics of magnetic skyrmions, Nat. Nanotechnol. **8**, 899 (2013).

[7] T. Fennell, P. P. Deen, A. R. Wildes, K. Schmalzl, D. Prabhakaran, A. T. Boothroyd, R. J. Aldus, D. F. McMorrow, and S. T. Bramwell, Magnetic coulomb phase in the spin ice ho2ti2o7, Science **326**, 415 (2009).

[8] S. T. Bramwell, S. R. Giblin, S. Calder, R. Aldus, D. Prabhakaran, and T. Fennell, Measurement of the charge and current of magnetic monopoles in spin ice, Nature (London) **461**, 956 (2009).

[9] D. J. P. Morris, D. A. Tennant, S. A. Grigera, B. Klemke, C. Castelnovo, R. Moessner, C. Czternasty, M. Meissner, K. C. Rule, J.-U. Hoffmann *et al.*, Dirac strings and magnetic monopoles in the spin ice $Dy_2Ti_2O_7$, Science **326**, 411 (2009).

[10] M. S. Rzchowski, Phase transitions in a kagome lattice of Josephson junctions, Phys. Rev. B **55**, 11745 (1997).

[11] I. M. Pop, K. Hasselbach, O. Buisson, W. Guichard, B. Pannetier, and I. Protopopov, Measurement of the current-phase relation in Josephson junction rhombi chains, Phys. Rev. B **78**, 104504 (2008).

[12] M. W. Johnson, M. H. S. Amin, S. Gildert, T. Lanting, F. Hamze, N. Dickson, R. Harris, A. J. Berkley, J. Johansson, P. Bunyk *et al.*, Quantum annealing with manufactured spins, Nature (London) **473**, 194 (2011).

[13] A. D. King, J. Carrasquilla, J. Raymond, I. Ozfidan, E. Andriyash, A. Berkley, M. Reis, T. Lanting, R. Harris, F. Altomare, K. Boothby, P. I. Bunyk, C. Enderud, A. Fréchette, E. Hoskinson, N. Ladizinsky, T. Oh, G. Poulin-Lamarre, C. Rich, Y. Sato, A. Yu. Smirnov, L. J. Swenson, M. H. Volkmann, J. Whittaker, J. Yao, E. Ladizinsky, M. W. Johnson, J. Hilton, and M. H. Amin, Observation of topological phenomena in a programmable lattice of 1,800 qubits, Nature (London) **560**, 456 (2018).

[14] J. W. Britton, B. C. Sawyer, A. C. Keith, C. C. J. Wang, J. K. Freericks, H. Uys, M. J. Biercuk, and J. J. Bollinger, Engineered two-dimensional ising interactions in a trapped-ion quantum simulator with hundreds of spins, Nature (London) **484**, 489 (2012).

[15] S. Weimann, L. Morales-Inostroza, B. Real, C. Cantillano, A. Szameit, and R. A. Vicencio, Transport in sawtooth photonic lattices, Opt. Lett. **41**, 2414 (2016).

[16] R. A. Vicencio, C. Cantillano, L. Morales-Inostroza, B. Real, C. Mejía-Cortés, S. Weimann, A. Szameit, and M. I. Molina, Observation of Localized States in Lieb Photonic Lattices, Phys. Rev. Lett. **114**, 245503 (2015).

[17] R. Moessner and A. P. Ramirez, Geometrical frustration, Phys. Today **59**, 24 (2006).

[18] J. Richter, O. Krupnitska, V. Baliha, T. Krokhmalskii, and O. Derzhko, Thermodynamic properties of $Ba_2CoSi_2O_6Cl_2$ in a strong magnetic field: Realization of flat-band physics in a highly frustrated quantum magnet, Phys. Rev. B **97**, 024405 (2018).

[19] A. Baniodeh, N. Magnani, Y. Lan, G. Buth, C. E. Anson, J. Richter, M. Affronte, J. Schnack, and A. K. Powell, High spin cycles: topping the spin record for a single molecule verging on quantum criticality, npj Quantum Mater. **3**, 10 (2018).

[20] S. Teitel and C. Jayaprakash, Phase transitions in frustrated two-dimensional XY models, Phys. Rev. B **27**, 598 (1983).

[21] L. N. Vu, M. S. Wistrom, and D. J. Van Harlingen, Imaging of magnetic vortices in superconducting networks and clusters by scanning squid microscopy, Appl. Phys. Lett. **63**, 1693 (1993).

[22] D. Valdez-Balderas and D. Stroud, Superconductivity versus phase separation, stripes, and checkerboard ordering: A two-dimensional Monte Carlo study, Phys. Rev. B **72**, 214501 (2005).

[23] R. Szymczak, M. Baran, R. Diduszko, J. Fink-Finowicki, M. Gutowska, A. Szewczyk, and H. Szymczak, Magnetic field-induced transitions in geometrically frustrated $Co_3V_2O_8$ single crystal, Phys. Rev. B **73**, 094425 (2006).

[24] B. Douçot and J. Vidal, Pairing of Cooper Pairs in a Fully Frustrated Josephson-Junction Chain, Phys. Rev. Lett. **88**, 227005 (2002).

[25] V. Cataudella and R. Fazio, Glassy dynamics of josephson arrays on a dice lattice, Europhys. Lett. **61**, 341 (2003).

[26] S. B. Lee, J.-S. Jeong, K. Hwang, and Y. B. Kim, Emergent quantum phases in a frustrated $J_1 - J_2$ Heisenberg model on the hyperhoneycomb lattice, Phys. Rev. B **90**, 134425 (2014).

[27] A. Andreanov and M. V. Fistul, Resonant frequencies and spatial correlations in frustrated arrays of josephson type nonlinear oscillators, J. Phys. A **52**, 105101 (2019).

[28] P. Jung, S. Butz, M. Marthaler, M. V. Fistul, J. Leppäkangas, V. P. Koshelets, and A. V. Ustinov, Multistability and switching in a superconducting metamaterial, Nat. Commun. **5**, 3730 (2014).

[29] K. V. Shulga, E. Il'ichev, M. V. Fistul, I. S. Besedin, S. Butz, O. V. Astafiev, U. Hübner, and A. V. Ustinov, Magnetically induced transparency of a quantum metamaterial composed of twin flux qubits, Nat. Commun. **9**, 150 (2018).

[30] A. K. Feofanov, V. A. Oboznov, V. V. Bol'ginov, J. Lisenfeld, S. Poletto, V. V. Ryazanov, A. N. Rossolenko, M. Khabipov, D. Balashov, A. B. Zorin, P. N. Dmitriev, V. P. Koshelets, and A. V. Ustinov, Implementation of superconductor/ferromagnet/superconductor π-shifters in superconducting digital and quantum circuits, Nat. Phys. **6**, 593 (2010).

[31] H. Hilgenkamp, Pi-phase shift josephson structures, Supercond. Sci. Technol. **21**, 034011 (2008).

[32] R. G. Dias and J. D. Gouveia, Origami rules for the construction of localized eigenstates of the Hubbard model in decorated lattices, Sci. Rep. **5**, 16852 (2015).

[33] P. W. Leung and V. Elser, Numerical studies of a 36-site kagome antiferromagnet, Phys. Rev. B **47**, 5459 (1993).

[34] S. E. Korshunov and B. Douçot, Fluctuations and Vortex-Pattern Ordering in the Fully Frustrated xy Model on a Honeycomb Lattice, Phys. Rev. Lett. **93**, 097003 (2004).

[35] S. E. Korshunov, Fluctuation-induced vortex pattern and its disordering in the fully frustrated xy model on a dice lattice, Phys. Rev. B **71**, 174501 (2005).

[36] J. T. Chalker, Geometrically frustrated antiferromagnets: Statistical mechanics and dynamics, in *Introduction to Frustrated Magnetism: Materials, Experiments, Theory*, edited by C. Lacroix, P. Mendels, and F. Mila (Springer, Berlin, 2011), pp. 3–22.

[37] J. Villain, R. Bidaux, J.-P. Carton, and R. Conte, Order as an effect of disorder, J. Phys. **41**, 1263 (1980).

[38] C. L. Henley, Ordering Due to Disorder in a Frustrated Vector Antiferromagnet, Phys. Rev. Lett. **62**, 2056 (1989).

[39] S. Prakash and C. L. Henley, Ordering due to disorder in dipolar magnets on two-dimensional lattices, Phys. Rev. B **42**, 6574 (1990).

[40] C. L. Henley, Effective Hamiltonians and dilution effects in kagome and related anti-ferromagnets, Can. J. Phys. **79**, 1307 (2001).

[41] A. Sen, K. Damle, and R. Moessner, Fractional Spin Textures in the Frustrated Magnet $SrCr_{9p}Ga_{12-9p}O_{19}$, Phys. Rev. Lett. **106**, 127203 (2011).